

Morphology and immunohistochemical characteristics of the otic ganglion in the chinchilla (*Chinchilla laniger* Molina)

Waldemar Sienkiewicz¹, Jacek Kuchinka², Agnieszka Dudek¹, Elżbieta Nowak²,
Jerzy Kaleczyc¹, Małgorzata Radzimska², Aleksander Szczurkowski³

¹Department of Animal Anatomy, Faculty of Veterinary Medicine, University of Warmia and Mazury in Olsztyn, Olsztyn, Poland

²Department of Medical Biology, Institute of Biology, Jan Kochanowski University in Kielce, Kielce, Poland

³Department of Pathomorphology, Histology and Forensic Medicine, Collegium Medicum, Jan Kochanowski University in Kielce, Poland

Abstract

Introduction. The available literature provides relatively little information on the morphology of the autonomic head ganglia in rodents including their neurochemical coding.

Material and methods. Morphological investigations of the otic ganglion of the chinchilla were performed using the modified acetylcholinesterase method. The cellular structure was investigated with histological techniques and neurochemical properties were studied with the double-labelling immunofluorescence method.

Results. Macromorphological investigations allowed the otic ganglion to be identified as a compact, oval agglomeration of neurons and nerve fibers. Multidimensional cross-sections revealed densely arranged neuronal perikarya and two populations of nerve cells differing in size were distinguished. The large cells (40–50 μm) accounted for about 80% of the neurons in the cross-sections. Moreover, a small number of intraganglionic nerve fibers was observed. Immunohistochemical staining revealed that over 85% of the neuronal cell bodies in the otic ganglion contained immunoreactivity to VACHT or ChAT. VIP-immunoreactive perikarya comprised approximately 10% of the ganglionic cells. Double staining revealed the presence of VACHT+ and NOS+ neurons which amounted to about 45% of the nerve cells in the otic ganglion. NOS+ only perikarya comprised approx. 15% of all the neurons. Immunoreactivity to enkephalins, substance P, somatostatin, and galanin was expressed in single nerve cell bodies and nerve fibers except numerous substance P+ intraganglionic nerve fibers. Some of them were stained also for CGRP. Single neurons stained for tyroxine hydroxylase.

Conclusions. Our results, compared with findings in other rodent species suggest the existence of interspecies differences in the morphology, cellular structure, and immunohistochemical properties of the head autonomic ganglia in mammals. (*Folia Histochemica et Cytobiologica* 2023, Vol. 61, No. 1, 17–25)

Keywords: chinchilla; otic ganglion; histochemistry; VACHT; ChAT; NOS; VIP; SP; double immunofluorescence

Correspondence address:

Jacek Kuchinka
Department of Medical Biology, Institute of Biology,
Jan Kochanowski University in Kielce, 7 Uniwersytecka St.,
25–406 Kielce, Poland
phone: +48 41 349-63-12
e-mail: jacek.kuchinka@ujk.edu.pl

Introduction

The otic ganglion as a peripheral head structure of the autonomic nervous system in terms of immunohistochemical properties is been insufficiently studied in small mammals. There are not enough literature data concerned with this structure. The present study was

thus designed to investigate the morphology and neurochemical properties of the otic ganglion in the chinchilla. The use of a modified classical histochemical method to localize cholinesterase activity has allowed autonomic cranial ganglia, including the otic ganglion, to be identified in many species of mammals [1, 2]. Acetylcholinesterase positive neurons (AChE+) were found in the otic ganglion in several animal species, such as dog [3], cat [4], spotted suslik [5], Egyptian spiny mouse [6], and rat [7]. Comparative anatomical studies performed in mammals indicate the presence of a significant relationship between the morphology, topography, and cellular structure of the parasympathetic head ganglia and the systematic position of the investigated rodents and domestic animals. Moreover, these ganglia display pronounced immunohistochemical differentiation between species. The specific immunohistochemical markers of parasympathetic structures belong to the enzyme that synthesizes acetylcholine, choline acetyltransferase (ChAT), and the specific neurotransmitter transporter protein, vesicular acetylcholine transporter (VAChT), responsible for loading acetylcholine into secretory vesicles in neurons, making it available for secretion. The presence of these two substances has been demonstrated in the otic ganglion of the rat [8–11] and pig [12]. The presence of markers identifying adrenergic neurons thyroxine hydroxylase (TH) and dopamine β -hydroxylase (DBH) was tested in a rat. A small number of neurons observed in this species, less than 5% of cells, were DBH positive while TH-positive neurons were absent [8]. Moreover, the expression of other biologically active substances, such as neuropeptide Y (NPY), vasoactive intestinal polypeptide (VIP), substance P (SP), and calcitonin gene-related peptide (CGRP), has been found in the otic ganglion of rat, pig, and human [8–10, 12, 13].

Chinchilla has been often used recently as a model species for the investigations of hearing and digestive system dysfunctions [14], innervation of the gastrointestinal system [15, 16] or innervation of the heart [17]. The available literature contains no information on the morphology and neurochemical properties of the otic ganglion in the chinchilla. The aim of this study was to investigate this part of the autonomic nervous system (ANS). The results will contribute to our knowledge of the organization of the ANS in mammals.

Material and methods

The investigations were carried out on twelve adults (10-month-old, weight 400–600 g) chinchillas (*Chinchilla laniger* Molina) of both sexes. These studies were approved in accordance with the appropriate Polish statute law on the protection of research

animals (Act for the Protection of Animals Used for Scientific or Educational Purpose 15 January 2015); studies on tissues obtained *post-mortem* do not require the approval of the Ethics Committee. The material was collected immediately after the industrial slaughter at a chinchilla fur farm. The mandibular nerves were exposed under a stereomicroscope, rinsed in physiological solution (NaCl 0.9%), and fixed for 30 min in 4% formaldehyde. Four individuals were used for morphological investigations using the modified acetylcholinesterase method [1, 2]. Procedure: 1. rinsing in distilled water; 2. pre-incubation in basic solution — pH 6.8 for 3 h (reagents: copper sulfate, glycine, magnesium chloride, maleic acid, sodium sulfate, 1 N sodium hydroxide); 3. incubation in solution for 1 h (reagents: acetylthiocholine iodide diluted in basic solution); 4. washing in saturated sodium sulfate; 5. placing of material in a mixture of thioacetamide with ammonia solution for 3 min; 6. washing in distilled water for 5 min; 7. subsequent placing of material in 30% acetic acid for 24 h; 8. the examined material was finally prepared, mounted in DPX medium and whole-mount specimens were studied under a binocular microscope. The activity of the pseudocholine nonspecific esterase was blocked using iso-OMPA (C₁₂H₃₂N₄O₃P₂ tetraiso-propylpyrophosphoramidate). Another four animals were used for the histological study. Once fixed in formaldehyde, the mandibular nerves after dehydration and clearing were embedded in paraffin (Paraplast plus) and in Historesine® (70-2218-501 Mounting Medium), cut with a microtome (Microm 325, Zeiss, Jena, Germany) for 3–5 μ m slides, stained according to the hematoxylin and eosin (H&E), methylene blue [18], and silvered methods [19]. Methylene blue staining: 1. collect the historesine sections on a drop of water on a glass slide and dry the sections on a heating plate (60–70°C); 2. leave the sections on the plate for an hour or longer; 3. flood the sample with methylene blue (1% in aqueous) for 1–3 minutes; 4. delicate wash in distilled water; 5. dehydrate; 6. clearing with xylene; 7. close with coverslip with DPX. Silver staining: 1. deparaffinized sections hydrated with distilled water 3 \times 3 min; 2. place sections in 50 mL 10% silver nitrate in dark at 37°C for 30 min; 3. wash 3 \times 3 min in dH₂O; 4. add concentrated ammonium hydroxide dropwise with stirring to the silver nitrate solution; 5. incubate sections in this solution for 15 min at 37°C; 6. wash sections in 0.1% ammonium hydroxide 3 \times for 2 min at room temperature; 7. add 350 μ L solution (0.2 mL 37% formaldehyde, 12 mL dH₂O, 12.5 μ L 20% nitric acid and 0.05 g citric acid) to the silver hydroxide solution; 7. stain sections in this solution for 10 min until they turn black; 8. wash in 0.1% ammonium hydroxide 3 \times for 2 min and dH₂O 3 \times for 2 min; 9. tone in 0.2% gold chloride for 5 min; 10. fix in 5% sodium thiosulfate for 1 min; 11. wash in dH₂O, dehydrate in alcohols then xylene and mount in DPX (mountant for histology, 44581 — SigmaAldrich, St. Luis, MO, USA).

Morphometry and photographic documentation were performed using a Nikon Digital Sight SD-L1 System and Nis-Elements 3.22 software with Nikon Eclipse 90i microscope (Nikon, Tokyo, Japan).

The final four animals used for the immunohistochemical investigations were transcardially perfused with 0.4 L of 4% ice-cold buffered paraformaldehyde, and the mandibular nerves were collected as described above. The tissues were postfixed by immersion in the same fixative for 2 hours, rinsed with phosphate buffer (pH 7.4) and transferred to 30% buffered sucrose solution for storage until further processing. The ganglia were cut into 12 μm -thick cryostat sections, which were processed for the double-labelling immunofluorescence method on slide-mounted sections. The sections were washed thrice for 10 min in PBS (phosphate-buffered saline), and incubated for 45 min. in 10% normal horse serum (NHS, Cappel, Warsaw, Poland) or normal goat serum (NGS, Cappel, Warsaw, Poland) in PBS containing 0.25% Triton X-100 (Sigma-Aldrich), and incubated overnight at room temperature (RT) with primary antibodies (Table 1) diluted in PBS containing 0.25% Triton X-100. After incubation with primary antiserum, the sections were washed three times for 10 min in PBS and further incubated with secondary antisera conjugated with fluorochrome Alexa Fluor 488 and Alexa Fluor 546 and 568 (Table 1) for 1 h at RT. After incubation, the sections were washed three times for 10 min in PBS, coverslipped with buffered glycerol, and examined under a confocal microscope (Zeiss, Wetzlar, Germany). Pairs of primary antibodies used for double staining: VIP/VACHT, NOS/VACHT, Met-ENK/ChAT, Leu-ENK/VACHT, GAL/ChAT, SOM/VACHT, SP/CGRP, TH/VACHT. Pairs of primary and secondary antibodies are listed in Table 2.

Sixty frozen sections from the four animals were used for the analysis. Every seventh section was used to avoid double counting of the same neurons. The number of immunoreactive perikarya was calculated as a percentage of all ganglionic cells on the whole cross-section area for each individual.

Staining specificity was controlled by preabsorption of a diluted antiserum with 20 $\mu\text{g}/\text{mL}$ of an appropriate antigen, which abolished the specific immunoreaction completely. In addition, experiments were carried out in which the primary antiserum was replaced by nonimmune serum or by PBS, to verify the specificity of immunoreactions. The results were described using veterinary anatomical nomenclature NAV 2017 [20].

Results

The histochemical investigations revealed extensive acetylcholinesterase (AChE) staining in the otic ganglion of the chinchilla. This allowed the ganglion to be identified as a compact, oval agglomeration of neurons and nerve fibers located inside the skull on the medial surface of the mandibular nerve, just above the oval foramen (Fig. 1A). The ganglion was 3–5 mm long, 2–3 mm wide and about 0.6 mm thick. The small petrosal nerve, as the parasympathetic radix, reaches the caudal part of the ganglion. In its course, a small aggregation (1 mm long and 0.4 mm wide) of neurocytes was observed. The maxillary artery ran below the ganglion crossing the mandibular nerve

more often on the medial side (70% of cases), and rarely on the lateral side (Fig. 1A).

Postganglionic fibers leaving the otic ganglion intensely stained for AChE. A delicate bundle of fibers left the superior surface of the structure and entered the trigeminal ganglion (Fig. 1A). A small aggregation of neurons in the course of this nerve was frequently observed.

The histological investigations confirmed the close contact between the otic ganglion and the mandibular nerve (Fig. 1A–D). Multidimensional cross-sections revealed densely arranged neuronal perikarya. Two populations of nerve cells differing in size could be distinguished: the large neurons with a diameter of 40–50 μm , and the small cells with a diameter of 28–25 μm (Fig. 1B, C). The large cells accounted for about 80% of the neurons in the otic ganglion cross-sections. The ganglionic neurons were surrounded by satellite cells with intensely stained nuclei (Fig. 1C). Moreover, a small number of intraganglionic nerve fibers was observed (Fig. 1D). The entire chinchilla otic ganglion was surrounded by a thin connective tissue capsule.

Immunohistochemical staining revealed that over 85% (70–95%, mean = 85%; SD \pm 4.68) of the neuronal cell bodies in the otic ganglion expressed immunoreactivity to VACHT (Fig. 2A), and a comparable number of the perikarya stained for ChAT (79–92%, mean = 86%; SD \pm 3.80) (Fig. 2C). These cells were mainly of the large type. VIP-immunoreactive (IR) perikarya made up approximately 10% of the ganglionic cells (7–13% mean = 10%; SD \pm 1.59); these were small or medium-sized neurons (Fig. 2A). Double staining revealed that approximately 20% (16–23%, mean = 19.93%; SD \pm 2.25) of the VIP-IR neurons were VACHT-negative (Fig. 2A). Intraganglionic VACHT-IR nerve fibers were numerous and often formed basket-like structures surrounding all the neuronal perikarya (Fig. 2A). VIP-positive nerves terminals were scarce. Double staining revealed the presence of VACHT- and NOS-positive neurons which amounted to about 45% (43–51%, mean = 45.27%; SD \pm 2.71) of the nerve cells in the otic ganglion. NOS-positive only perikarya made up approximately 15% (12–19% mean = 15.21%; SD \pm 1.91) of all the neurons (Fig. 2B); these neurons were cells of the small type, whereas double-stained neurons had medium-size and large perikarya. Only a few intraganglionic NOS-positive nerve fibers were encountered.

Immunoreactivity to enkephalin (ENK) was expressed in the nerve cell bodies and nerve fibers. Staining against Met-ENK revealed only 3–4 nerve cell bodies per section that were immunoreactive to this peptide (Fig. 2C); approximately half of these were si-

Table 1. Antisera used in the study

| Primary antisera | | | | | |
|------------------------------|-----------------|------------|----------|-------------------------------|--|
| Antigen | Host | Type | Dilution | Cat. No. | Supplier |
| ChAT | Goat | Polyclonal | 1:50 | AB144P | Millipore, Temecula, CA, USA |
| VACHT | Rabbit | Polyclonal | 1:4000 | V5387 | Sigma-Aldrich, Saint Louis, MI, USA |
| TH | Mouse | Monoclonal | 1:50 | T2928 | Sigma-Aldrich, Saint Louis, MI, USA |
| VIP | Mouse | Monoclonal | 1:500 | MaVIP | East Acres Biologicals, Southbridge, MA, USA |
| CGRP | Rabbit | Polyclonal | 1:2000 | 11535 | Cappel, Aurora, OH, USA |
| SP | Rat | Monoclonal | 1:150 | 8450-0505 | AbD Serotec, Hercules, CA, USA |
| GAL | Rabbit | Polyclonal | 1:2000 | RIN 7153 | Peninsula Lab., Switzerland |
| NOS | Mouse | Monoclonal | 1:100 | N2280 | Sigma-Aldrich, Saint Louis, MI, USA |
| Leu-5-Enk | Rabbit | Polyclonal | 1:500 | RPN 1552 | Amersham, UK |
| Met-5-Enk | Rabbit | Polyclonal | 1:500 | RPN 1562 | Amersham, UK |
| SOM | Rat | Polyclonal | 1:500 | MAB354 | Millipore, Temecula, CA, USA |
| Secondary antisera | | | | | |
| Host | Fluorochrom | Dilution | Code | Supplier | |
| Donkey-anti-goat IgG (H+L) | Alexa Fluor 546 | 1:500 | A11056 | Invitrogen, Carlsbad, CA, USA | |
| Donkey-anti-rabbit IgG (H+L) | Alexa Fluor 488 | 1:500 | A21206 | Invitrogen, Carlsbad, CA, USA | |
| Donkey-anti-mouse IgG (H+L) | Alexa Fluor 488 | 1:500 | A21202 | Invitrogen, Carlsbad, CA, USA | |
| Goat-anti-mouse IgG (H+L) | Alexa Fluor 488 | 1:500 | A11001 | Invitrogen, Carlsbad, CA, USA | |
| Goat-anti-rabbit IgG (H+L) | Alexa Fluor 568 | 1:500 | A11011 | Invitrogen, Carlsbad, CA, USA | |
| Goat-anti-rat IgG (H+L) | Alexa Fluor 488 | 1:500 | A-11006 | Invitrogen, Carlsbad, CA, USA | |

Abbreviations: CGRP — calcitonin gene-related peptide; ChAT — choline acetyltransferase; GAL — galanin; Leu-5-ENK — Leu-enkephalin; Met-5-ENK — Met-enkephalin; NOS — nitric oxide synthase; SOM — somatostatin; SP — substance P; TH — tyrosine hydroxylase; VACHT — vesicular acetylcholine transporter; VIP — vasoactive intestinal polypeptide.

multaneously ChAT-positive (Fig. 2C). Intraganglionic Met-ENK-IR nerve fibers were moderate in number (Fig. 2C). Leu-ENK-immunoreactivity was found in the cell bodies of one or two neurons per section. These perikarya were simultaneously VACHT-positive. The Leu-ENK-IR nerve fibers were very scarce.

Galanin (GAL)-IR neurons also occurred only individually (3–4 per section) and were stained for ChAT. GAL-positive nerves were very scarce and delicate. Few somatostatin (SOM)-positive only nerve cell bodies were encountered in the ganglion (Fig. 2D). Intraganglionic SOM-IR nerves were solitary and delicate. SP-positive intraganglionic nerve fibers were numerous and some of them were also stained for CGRP (Fig. 2E). SP-IR nerves formed basket-like structures surrounding nerve cell bodies. CGRP-immunoreactivity was found in nerve fibers that were less numerous than those that stained for SP. The vast majority of these were also SP-positive; individual nerve fibers contained only CGRP-immunoreactivity. Immunoreactivity to SP was also found in 1–2 neurons per section (Fig. 2E). Also, 3–4 neurons per section were stained for tyrosine hydroxylase; these were small, intensely stained, and scattered throughout the ganglion (Fig. 2F).

Table 2. Primary and secondary antisera used in the study

| Primary antisera | Host of primary antisera | Host of secondary antisera | Fluorochrom |
|------------------|--------------------------|-------------------------------|-----------------|
| ChAT | Goat | Donkey-anti-goat IgG (H + L) | Alexa Fluor 546 |
| VACHT | Rabbit | Goat-anti-rabbit IgG (H + L) | Alexa Fluor 568 |
| TH | Mouse | Donkey-anti-mouse IgG (H + L) | Alexa Fluor 488 |
| VIP | Mouse | Donkey-anti-mouse IgG | Alexa Fluor 488 |
| CGRP | Rabbit | Goat-anti-rabbit IgG (H + L) | Alexa Fluor 568 |
| SP | Rat | Goat-anti-rat IgG (H + L) | Alexa Fluor 488 |
| GAL | Rabbit | Donkey-anti-rabbit IgG | Alexa Fluor 488 |
| NOS | Mouse | Goat-anti-mouse IgG (H + L) | Alexa Fluor 488 |
| Leu-5-Enk | Rabbit | Donkey-anti-rabbit IgG | Alexa Fluor 488 |
| Met-5-Enk | Rabbit | Donkey-anti-rabbit IgG | Alexa Fluor 488 |
| SOM | Rat | Goat-anti-rat IgG (H + L) | Alexa Fluor 488 |

Abbreviations: see descriptions under Table 1.

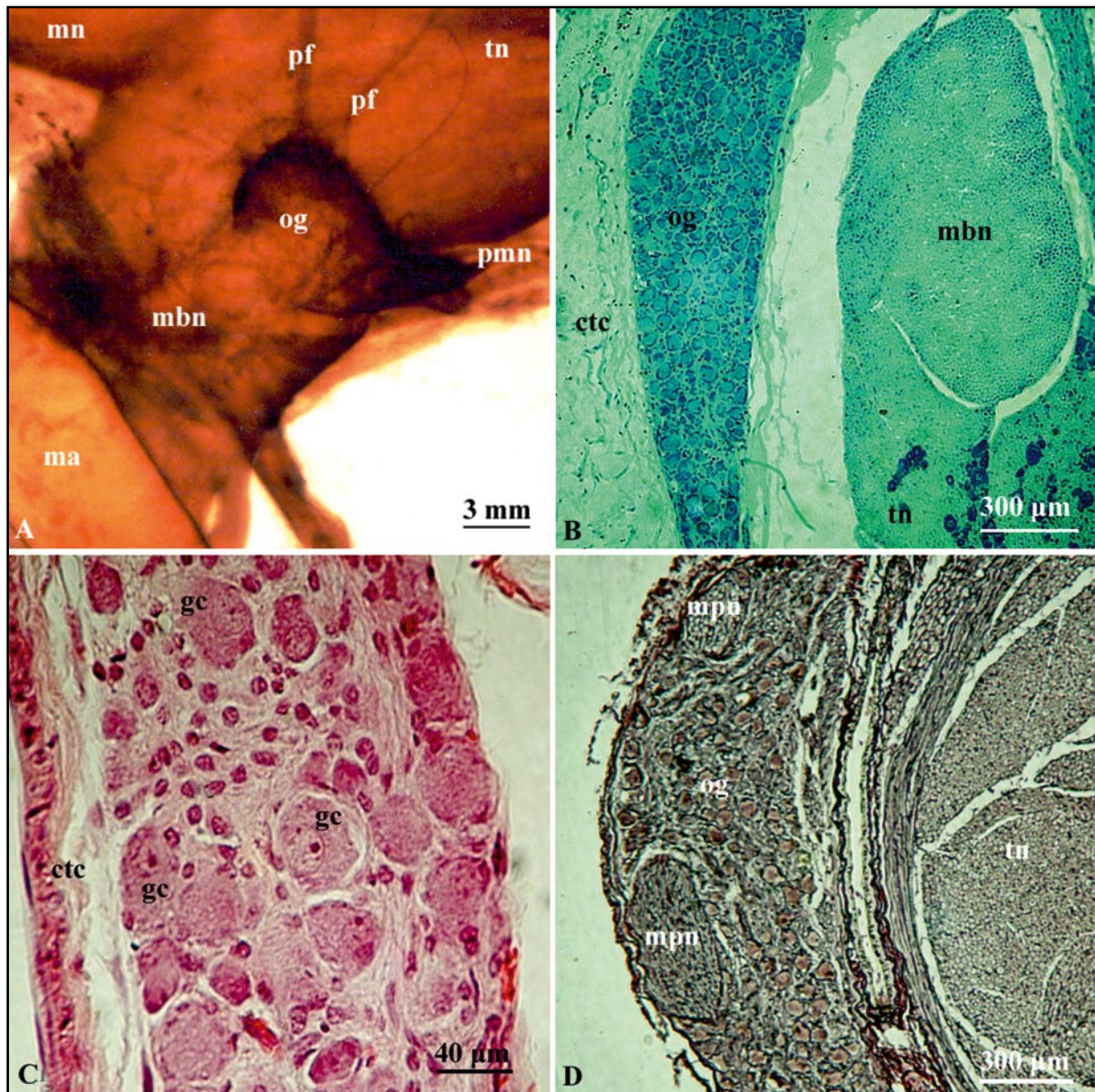


Figure 1. Morphology, topography, and cellular structure of the otic ganglion in chinchilla. **A.** Morphology of the otic ganglion in chinchilla. Thiocholine method. **B.** Cross-section through the otic ganglion in the chinchilla. Methylene blue staining. **C.** Cross-section through the central part of the otic ganglion in the chinchilla. H&E staining. **D.** Cross-section through the otic ganglion in chinchilla. Silver staining method. Abbreviations: ctc — connective tissue capsule; gc — ganglionic cells; ma — maxillary artery; mbn — mandibular nerve; mn — maxillary nerve; og — otic ganglion; pf — postganglionic fibers; pmn — minor petrosal nerve; tn — trigeminal nerve.

Our results did not reveal any sex differences.

Discussion

Our analysis of the topography of the otic ganglion in dog [3] and guinea pig [21] revealed a close relationship between two anatomical structures: the mandibular nerve and the maxillary artery. In most small mammalian species that have been investigated, the maxillary artery runs along the medial size of

the mandibular nerve. In this case, the otic ganglion was located on the medial surface of the mandibular nerve or had direct contact with the maxillary artery [3, 22–25]. The otic ganglion in the chinchilla is an intracranial structure found on the medial surface of the mandibular nerve, and only postganglionic fibers run parallel to the maxillary artery.

In most mammals, the otic ganglion is a single compact aggregation of neurons. This arrangement has been observed in small mammals, including rabbit [26], dog,

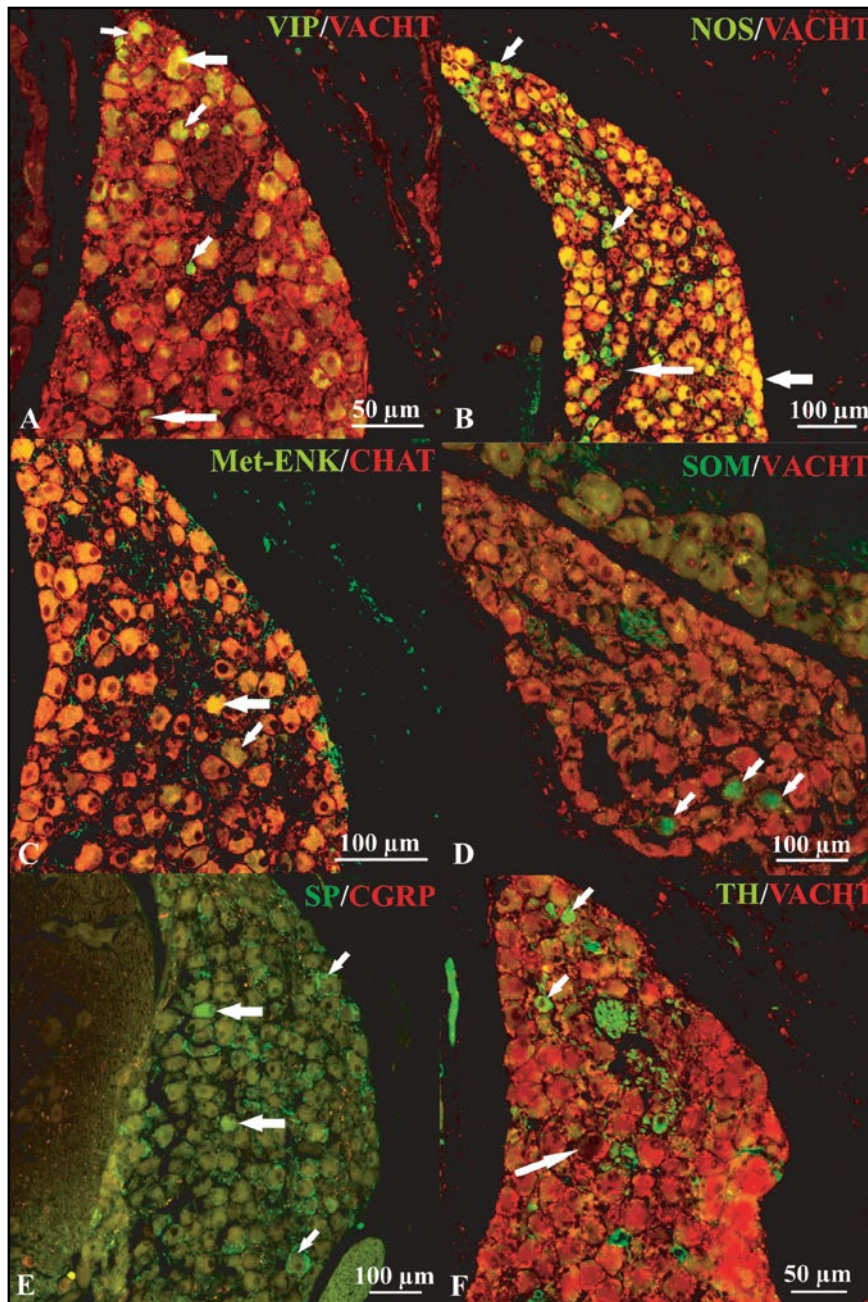


Figure 2. Immunohistochemical coding of the otic ganglion in chinchilla. **A.** Section from the otic ganglion stained with antibodies against VACHT (red) and VIP (green). The majority of the neurons exhibited immunoreactivity to VACHT, and a number of them were also stained for VIP. Some neurons displayed immunoreactivity to VIP only (examples indicated by small arrows). The vast majority of VIP-IR neurons is also VACHT-IR (example indicated by large arrow). Only single neurons are immunonegative for both studied substances (long arrow). Very numerous VACHT-immunoreactive nerve fibers formed “basket-like structures” surrounding perikarya. **B.** Section from the otic ganglion stained with antibodies against VACHT (red) and NOS (green). Over half of the neurons contained NOS-immunoreactivity, whereas double stained nerve cell bodies comprised approx. 45% of all the neurons (examples indicated by large arrow). Neurons stained for NOS only are indicated by small arrows. Single neurons are immunonegative for both studied substances (long arrow). **C.** ChAT- (red) and Met-ENK-positive (green) nerve structures in the otic ganglion. The vast majority of ganglionic cells were ChAT-positive. Single neurons contained Met-ENK-immunoreactivity (arrows) and some neuronal somata were simultaneously ChAT-positive (large arrow). Part of the neurons contained only Met-ENK-IR (small arrow). Note the presence of Met-ENK-IR ganglionic nerve fibers. **D.** VACHT- (red) or SOM-positive (green) neurons in the otic ganglion. SOM-immunoreactivity was restricted to single perikarya (small arrows) and fine nerve fibers. **E.** CGRP- (red) and/or SP-positive (green) structures in the otic ganglion. Immunoreactivity to SP was present in single neurons (large arrows). Note the presence of a moderate in number SP-positive (green) and/or CGRP-positive (yellow/red) nerve fibers. **F.** VACHT- (red) or TH-positive (green) neurons in the otic ganglion. Immunoreactivity to TH was present in single perikarya (small arrows). Single neurons are immunonegative for both studied substances (long arrow).

guinea pig, hedgehog [3, 21, 23], mouse, rat, hamster, midday gerbil [24, 25], spotted suslik [5], Egyptian spiny mouse [6], and larger mammals [27–30].

Sometimes the otic ganglion forms a ring-shaped structure encircling the maxillary artery [25]. In some species, the otic ganglion consists of several interconnected nerve cell clusters. This morphological form has been described in the wild pig [29], dog [3], goat, and sheep [30], whereas in cats the ganglion is composed of one main cluster of neurons and about ten small additional ganglia [4]. The otic ganglion in the chinchilla represents a single agglomeration of neurons and only one small additional ganglion was found, associated with the small petrosal nerve.

This relatively small ganglion is an important source of nerve fibers contributing to the innervation of many organs, including the parotid gland, buccal glands, and the blood vessels supplying the brain, lower lip, and gingiva [31, 32]. Previous studies have shown that the vast majority of neurons in the otic ganglion are cholinergic in nature [12]. Correspondingly, in the chinchilla 85% of these neurons are immunoreactive to ChAT or VAcHT. The presence of catecholaminergic (TH-positive) neurons within this parasympathetic ganglion may be considered somewhat surprising. This small neuronal population probably represents a kind of the “developmental relic”, consisting of not fully functional adrenergic nerve cells. This has been suggested in relation to catecholaminergic neurons in the porcine ciliary and pterygopalatine ganglia [33, 34], and in the pterygopalatine ganglion of the chinchilla [35]. However, such observations concerning different parasympathetic ganglia have previously also been made regarding pig [12, 33, 34] and rat [32], as well as human, monkey, guinea pig, ferret, dog, and cat [36–40]. Catecholaminergic neurons usually constitute small subpopulations in these ganglia, but they are much more numerous in human (23% ganglionic neurons) [38] and monkey (68% ganglionic neurons) [37] ciliary ganglia.

Our study showed that VIP-positive neurons constituted 10% of all ganglionic neurons. Few VIP-immunoreactive neurons were found in the porcine and rat otic ganglion [8, 12], while in the human otic ganglion over 90% of neurons are VIP-positive [39]. In the chinchilla pterygopalatine ganglion, a large population (40%) of VIP-immunoreactive neurons was found [35], whereas in the pig, all neurons in this ganglion were VIP-positive [34]. We also found that in chinchilla many (60%) ganglionic neurons stained for NOS. A large (80%) population of NOS-positive neurons has been found in the human otic ganglion [39]. The pterygopalatine ganglion in the chinchilla also makes up a large population (42%) of NOS-IR

neurons [35], whereas all the neurons are NOS-positive in the porcine pterygopalatine ganglion [34].

This study has revealed small populations of neurons immunoreactive to Met-enkephalin and Leu-enkephalin. The expression of opioid peptides in otic ganglion neurons has been studied in the guinea pig [40, 41] and, unlike our results on the chinchilla, a large (35%) subpopulation of the opioidergic neurons was found [41]. Individual GAL-IR and SOM-IR neurons were found in the porcine otic ganglion [12]. These findings correspond with our results.

In our study, we observed a dense network of VAcHT-immunoreactive nerve terminals, frequently forming basket-like structures surrounding the nerve cell bodies. The nerve fibers that were immunoreactive to SP and CGRP were also relatively numerous. It can be assumed that the VAcHT-positive nerve fibers represent two populations of nerve terminals: the first one consists of postganglionic nerve fibers originating from the ganglion, and the second consists of preganglionic nerves originating from the parasympathetic nucleus of the glossopharyngeal nerve. SP and/or CGRP-positive nerve fibers are probably sensory in nature and most likely represent collaterals of dendrites from the mandibular nerve which pass through the otic ganglion [8].

A comparison of previous findings with our present results suggests the existence of profound interspecies differences in the immunohistochemical characteristics of nerve structures of the otic ganglion. Further studies should be undertaken to clarify the functional significance of these differences.

Acknowledgements

The authors would like to thank Ms. M. Marczak for her excellent technical assistance.

References

1. Gienc J. The application of the histochemical method in the anatomical studies on the parasympathetic ganglia and nerve bundles of postganglionic axons in the sublingual region of some mammals. *Zool Pol.* 1977; 26: 187–192.
2. Tsuji S, Larabi Y. A modification of thiocholine-ferricyanide method of Karnovsky and Roots for localization of acetylcholinesterase activity without interference by Koelle's copper thiocholine iodide precipitate. *Histochemistry.* 1983; 78(3): 317–323, doi: [10.1007/BF00496619](https://doi.org/10.1007/BF00496619), indexed in Pubmed: [6193086](https://pubmed.ncbi.nlm.nih.gov/6193086/).
3. Gienc J, Kuder T. Otic ganglion in dog. Topography and macroscopic structure. *Folia Morphol (Warsz).* 1983; 42(1): 31–40, indexed in Pubmed: [6603394](https://pubmed.ncbi.nlm.nih.gov/6603394/).
4. Kuchiiwa S, Kuchiiwa T, Nonaka S, et al. Facial nerve parasympathetic preganglionic afferents to the accessory otic ganglia by way of the chorda tympani nerve in the cat. *Anat Embryol (Berl).* 1998; 197(5): 377–382, doi: [10.1007/s004290050148](https://doi.org/10.1007/s004290050148), indexed in Pubmed: [9623671](https://pubmed.ncbi.nlm.nih.gov/9623671/).

5. Szczurkowski A. Morphology, topography and cytoarchitectonics of the otic ganglion in the spotted suslik (*Spermophilus suslicus*, Gldenstaedt 1770). *Annals of Anatomy - Anatomischer Anzeiger*. 1999; 181(4): 409–411, doi: [10.1016/s0940-9602\(99\)80139-3](https://doi.org/10.1016/s0940-9602(99)80139-3).
6. Szczurkowski A, Kuder T, Nowak E, et al. Morphology, topography and cytoarchitectonics of the otic ganglion in Egyptian spiny mouse (*Acomys cahirinus*, Desmarest). *Folia Morphol (Warsz)*. 2001; 60(1): 61–64, indexed in Pubmed: [11234700](https://pubmed.ncbi.nlm.nih.gov/11234700/).
7. Shimizu T. Distribution and pathway of the cerebrovascular nerve fibers from the otic ganglion in the rat: anterograde tracing study. *J Auton Nerv Syst*. 1994; 49(1): 47–54, doi: [10.1016/0165-1838\(94\)90019-1](https://doi.org/10.1016/0165-1838(94)90019-1), indexed in Pubmed: [7525688](https://pubmed.ncbi.nlm.nih.gov/7525688/).
8. Hardebo JE, Suzuki N, Ekblad E, et al. Vasoactive intestinal polypeptide and acetylcholine coexist with neuropeptide Y, dopamine-beta-hydroxylase, tyrosine hydroxylase, substance P or calcitonin gene-related peptide in neuronal subpopulations in cranial parasympathetic ganglia of rat. *Cell Tissue Res*. 1992; 267(2): 291–300, doi: [10.1007/BF00302967](https://doi.org/10.1007/BF00302967), indexed in Pubmed: [1350946](https://pubmed.ncbi.nlm.nih.gov/1350946/).
9. Leblanc GG, Trimmer BA, Landis SC. Neuropeptide Y-like immunoreactivity in rat cranial parasympathetic neurons: coexistence with vasoactive intestinal peptide and choline acetyltransferase. *Proc Natl Acad Sci U S A*. 1987; 84(10): 3511–3515, doi: [10.1073/pnas.84.10.3511](https://doi.org/10.1073/pnas.84.10.3511), indexed in Pubmed: [3554241](https://pubmed.ncbi.nlm.nih.gov/3554241/).
10. Suzuki N, Hardebo JE, Khrstrm J, et al. Neuropeptide Y Co-Exists with Vasoactive Intestinal Polypeptide and Acetylcholine in Parasympathetic Cerebrovascular Nerves Originating in the Sphenopalatine, OTIC, and Internal Carotid Ganglia of the Rat. *Neuroscience*. 1990; 36(2): 507–519, doi: [10.1016/0306-4522\(90\)90001-7](https://doi.org/10.1016/0306-4522(90)90001-7).
11. Suzuki N, Hardebo JE, Owman C. Origins and pathways of choline acetyltransferase-positive parasympathetic nerve fibers to cerebral vessels in rat. *J Cereb Blood Flow Metab*. 1990; 10(3): 399–408, doi: [10.1038/jcbfm.1990.70](https://doi.org/10.1038/jcbfm.1990.70), indexed in Pubmed: [2329127](https://pubmed.ncbi.nlm.nih.gov/2329127/).
12. Lakomy M, Kaleczyc J, Wasowicz K, et al. Immunohistochemical study of the otic ganglion in the pig. *Pol J Vet Sci*. 2002; 5(4): 257–262, indexed in Pubmed: [12512560](https://pubmed.ncbi.nlm.nih.gov/12512560/).
13. Ayer-LeLievre C, Seiger Å. Substance P-like immunoreactivity in developing cranial parasympathetic neurons of the rat. *Int J Devl Neuroscience*. 2003; 3(3): 267–277, doi: [10.1016/0736-5748\(85\)90031-0](https://doi.org/10.1016/0736-5748(85)90031-0).
14. Suckow MA, Stevens KA, Wilson RP. The laboratory rabbit, guinea pig, hamster, and other rodents. 1st ed. Saunders: Elsevier, Amsterdam 2012.
15. Nowak E. Organization of the innervation of the oesophagus and stomach in chinchilla (*Chinchilla laniger*, Molina). *Folia Histochem Cytobiol*. 2013; 51(2): 115–120, doi: [10.5603/FHC.2013.0018](https://doi.org/10.5603/FHC.2013.0018), indexed in Pubmed: [23907940](https://pubmed.ncbi.nlm.nih.gov/23907940/).
16. Radzimirska M, Kuchinka J, Nowak E, et al. Cholinergic and adrenergic innervation of the pancreas in chinchilla (*Chinchilla laniger* Molina). *Folia Histochem Cytobiol*. 2020; 58(1): 54–60, doi: [10.5603/FHC.a2020.0005](https://doi.org/10.5603/FHC.a2020.0005), indexed in Pubmed: [32202307](https://pubmed.ncbi.nlm.nih.gov/32202307/).
17. Radzimirska M, Kuchinka J, Kuder T, et al. Distribution and neurochemical characteristic of the cardiac nerve structures in the heart of chinchilla (*Chinchilla laniger* Molina). *Folia Histochem Cytobiol*. 2021; 59(3): 157–166, doi: [10.5603/FHC.a2021.0021](https://doi.org/10.5603/FHC.a2021.0021), indexed in Pubmed: [34581422](https://pubmed.ncbi.nlm.nih.gov/34581422/).
18. Highley JR, Sullivan N. Neuropathology and muscle biopsy techniques. In: Suvarna SK, Layton C, Bancroft JD. ed. *Bancroft's theory and practice of histological techniques*. 8th ed. Elsevier, Amsterdam 2019: 306–336.
19. Zawistowski S. *Technika histologiczna, histologia oraz podstawy histopatologii*. PZWL, Warszawa 1986.
20. International Committee on Veterinary Gross Anatomical Nomenclature ICVGAN. *Nomina Anatomica Veterinaria*. 6th ed. The Editorial Committee, Hanover, Ghent, Columbia, Rio de Janeiro 2017.
21. Gienc J, Kuder T. Morphology and topography of the otic ganglion in guinea pig detected with thiocholine technique. *Folia Morphol (Warsz)*. 1980; 39(1): 79–85, indexed in Pubmed: [6965653](https://pubmed.ncbi.nlm.nih.gov/6965653/).
22. Fischbach I, Dudzińska B. Topography of the otic ganglion in rabbit. [Topografia zwoju usznego u krlika, in Polish]. *Folia Morphol (Warsz)*. 1970; 29(4): 241–247.
23. Gienc J, Kuder T, Szczurkowski A. Parasympathetic Ganglia in the head of western hedgehog (*Erinaceus europaeus*). I. Otic ganglion. *Acta Theriologica*. 1988; 33: 115–120, plates 5–6, doi: [10.4098/at.arch.88-10](https://doi.org/10.4098/at.arch.88-10).
24. Kuder T, Kuder T, Kuder T. Comparative morphology and topography of cranial parasympathetic ganglia connected with the trigeminal nerve in mouse, rat and hamster (*Mus musculus* L. 1759, *Rattus norvegicus* B. 1769, *Mesocricetus aureatus* W. 1839). Part I. Otic ganglion. *Folia Morphol (Warsz)*. 1983; 42(3): 187–197, indexed in Pubmed: [6607866](https://pubmed.ncbi.nlm.nih.gov/6607866/).
25. Kuder T. Topography and macroscopic structure of parasympathetic ganglia connected with the trigeminal nerve in midday gerbil (*Meriones meridianus* - Mammalia: Rodentia). *Acta Biol Cracow Zool*. 1985; 27: 61–71.
26. Dixon JS. The fine structure of parasympathetic nerve cells in the otic ganglia of the rabbit. *Anat Rec*. 1966; 156(3): 239–251, doi: [10.1002/ar.1091560302](https://doi.org/10.1002/ar.1091560302).
27. Godinho H. A comparative anatomical study of the cranial nerves in goat, sheep and bovine (*Capra hircus*, *Ovis aries* and *Bos taurus*): their distribution and related autonomic components [a dissertation]. Iowa State University, Ames-Iowa. 1968, doi: [10.31274/rtd-180814-889](https://doi.org/10.31274/rtd-180814-889).
28. Petela L. Topography of the trigeminal nerve in cattle. Part III. Mandibular nerve. [Topografia nerwu trjdzielnego u bydła. Czść III. Nerw zuchwowy. In Polish]. *Pol Arch Vet*. 1974; 17: 559–580.
29. Petela L. The trigeminal nerve in boar (*Sus scrofa* L. 1758). [Nerw trjdzielny u dzika (*Sus scrofa* L. 1758), in Polish]. *Zesz Nauk AR Wroclaw*. 1979; 17: 1–55.
30. Kovikova LP. The otic ganglion in domestic animals. [Usnoj uzel - gln. oticum domasnich zivotnych]. *Ucenyje Zap Viteb Vet Inst*. 1958; 16: 11–114.
31. Edvinsson L, Elss T, Suzuki N, et al. Origin and Co-localization of nitric oxide synthase, CGRP, PACAP, and VIP in the cerebral circulation of the rat. *Microsc Res Tech*. 2001; 53(3): 221–228, doi: [10.1002/jemt.1086](https://doi.org/10.1002/jemt.1086), indexed in Pubmed: [11301497](https://pubmed.ncbi.nlm.nih.gov/11301497/).
32. Suzuki N, Shimizu T, Takao M, et al. Occurrence and distribution of substance P receptors in the cerebral blood vessels of the rat. *Brain Res*. 1999; 830(2): 372–378, doi: [10.1016/s0006-8993\(99\)01386-4](https://doi.org/10.1016/s0006-8993(99)01386-4), indexed in Pubmed: [10366695](https://pubmed.ncbi.nlm.nih.gov/10366695/).
33. Kaleczyc J, Juranek J, Całka J, et al. Immunohistochemical characterization of neurons in the porcine ciliary ganglion. *Pol J Vet Sci*. 2005; 8(1): 65–72, indexed in Pubmed: [15794476](https://pubmed.ncbi.nlm.nih.gov/15794476/).
34. Podlasz P, Wsowicz K, Kaleczyc J, et al. Localization of immunoreactivities for neuropeptides and neurotransmitter-synthesizing enzymes in the pterygopalatine ganglion of the pig. *Veterinrni Medicina*. 2012; 48(4): 99–107, doi: [10.17221/5756-vetmed](https://doi.org/10.17221/5756-vetmed).
35. Szczurkowski A, Sienkiewicz W, Kuchinka J, et al. Morphology and immunohistochemical characteristics of the pterygopalatine ganglion in the chinchilla (*Chinchilla laniger*, Molina). *Pol J Vet Sci*. 2013; 16(2): 359–368, doi: [10.2478/pjvs-2013-0048](https://doi.org/10.2478/pjvs-2013-0048), indexed in Pubmed: [23971205](https://pubmed.ncbi.nlm.nih.gov/23971205/).
36. Landis SC, Jackson PC, Fredieu JR, et al. Catecholaminergic properties of cholinergic neurons and synapses in adult rat ciliary ganglion. *J Neurosci*. 1987; 7(11): 3574–3587, doi: [10.1523/JNEUROSCI.07-11-03574.1987](https://doi.org/10.1523/JNEUROSCI.07-11-03574.1987), indexed in Pubmed: [2890721](https://pubmed.ncbi.nlm.nih.gov/2890721/).

37. Uemura Y, Sugimoto T, Nomura S, et al. Tyrosine hydroxylase-like immunoreactivity and catecholamine fluorescence in ciliary ganglion neurons. *Brain Res.* 1987; 416(1): 200–203, doi: [10.1016/0304-3940\(86\)90547-1](https://doi.org/10.1016/0304-3940(86)90547-1), indexed in Pubmed: [3537849](https://pubmed.ncbi.nlm.nih.gov/3537849/).
38. Kirch W, Neuhuber W, Tamm ER. Immunohistochemical localization of neuropeptides in the human ciliary ganglion. *Brain Res.* 1995; 681(1-2): 229–234, doi: [10.1016/0006-8993\(95\)00299-6](https://doi.org/10.1016/0006-8993(95)00299-6), indexed in Pubmed: [7552287](https://pubmed.ncbi.nlm.nih.gov/7552287/).
39. Uddman R, Tajti J, Möller S, et al. Neuronal messengers and peptide receptors in the human sphenopalatine and otic ganglia. *Brain Research.* 1999; 826(2): 193–199, doi: [10.1016/S0006-8993\(99\)01260-3](https://doi.org/10.1016/S0006-8993(99)01260-3).
40. Gibbins IL. Target-related patterns of co-existence of neuropeptide Y, vasoactive intestinal peptide, enkephalin and substance P in cranial parasympathetic neurons innervating the facial skin and exocrine glands of guinea-pigs. *Neuroscience.* 1990; 38(2): 541–560, doi: [10.1016/0306-4522\(90\)90049-a](https://doi.org/10.1016/0306-4522(90)90049-a).
41. Shimizu T, Morris JL, Gibbins IL. Expression of immunoreactivity to neurokinin-1 receptor by subsets of cranial parasympathetic neurons: correlation with neuropeptides, nitric oxide synthase, and pathways. *Exp Neurol.* 2001; 172(2): 293–306, doi: [10.1006/exnr.2001.7799](https://doi.org/10.1006/exnr.2001.7799), indexed in Pubmed: [11716554](https://pubmed.ncbi.nlm.nih.gov/11716554/).

Submitted: 7 October, 2022

Accepted after reviews: 2 January, 2023

Available as AoP: 23 January, 2023